

# RAFT Synthesis of Poly(*N*-isopropylacrylamide) and Poly(methacrylic acid) Homopolymers and Block Copolymers: Kinetics and Characterization

Chiming Yang,<sup>1,2</sup> Yu-Ling Cheng<sup>1,2</sup>

<sup>1</sup>Department of Chemical Engineering and Applied Chemistry, University of Toronto, Toronto, Ontario M5S 3E5, Canada

<sup>2</sup>Institute of Biomaterials and Biomedical Engineering, University of Toronto, Toronto, Ontario M5S 3G9, Canada

Received 26 January 2006; accepted 7 March 2006

DOI 10.1002/app.24415

Published online in Wiley InterScience (www.interscience.wiley.com).

**ABSTRACT:** Reversible addition-fragmentation chain transfer (RAFT) polymerization was used successfully to synthesize temperature-responsive poly(*N*-isopropylacrylamide) (PNIPAAm), poly(methacrylic acid) (PMAA), and their temperature-responsive block copolymers. Detailed RAFT polymerization kinetics of the homopolymers was studied. PNIPAAm and PMAA homopolymerization showed living characteristics that include a linear relationship between  $\bar{M}_n$  and conversion, controlled molecular weights, and relatively narrow molecular weight distribution (PDI < 1.3). Furthermore, the homopolymers can be reactivated to produce block copolymers. The RAFT agent, carboxymethyl dithiobenzoate (CMDB), proved to control molecular weight and PDI. As the RAFT agent concentration

increases, molecular weight and PDI decreased. However, CMDB showed evidence of having a relatively low chain transfer constant as well as degradation during polymerization. Solution of the block copolymers in phosphate buffered saline displayed temperature reversible characteristics at a lower critical solution temperature (LCST) transition of 31°C. A 5 wt % solution of the block copolymers form thermoreversible gels by a self-assembly mechanism above the LCST. © 2006 Wiley Periodicals, Inc. *J Appl Polym Sci* 102: 1191–1201, 2006

**Key words:** stimuli-responsive polymer; block copolymers; reversible addition-fragmentation chain transfer (RAFT); polymerization kinetics; *N*-isopropylacrylamide

## INTRODUCTION

Stimuli-responsive polymers have attracted attention over the past two decades because of both intrinsic scientific interest and their potential in biomedical, pharmaceutical, and tissue engineering applications. Poly(*N*-isopropylacrylamide) (PNIPAAm) is well known to exhibit a reversible temperature-responsive phase transition at a lower critical solution temperature (LCST) of ~32°C in aqueous solutions.<sup>1</sup> Below its LCST, PNIPAAm is water soluble and hydrophilic. Above its LCST, PNIPAAm undergoes a phase transition to an insoluble, hydrophobic aggregate. Poly(methacrylic acid) (PMAA) is a weak polyelectrolyte that has been shown to promote local angiogenesis (i.e., promote blood vessels formation).<sup>2</sup> The mechanism of action relates to PMAA's ability to act as a sink for endogenous growth factors, thereby stabilizing them (in analogous to components of the extracellular matrix) and permitting their slow release over time.<sup>2</sup> Thus,

block copolymers of temperature-responsive PNIPAAm and bioactive PMAA create systems that respond to temperature and are possibly therapeutic. Furthermore, block copolymers of PNIPAAm and PMAA may form temperature-dependent aggregates or gels by a self-assembly mechanism.<sup>3,4</sup>

Reversible addition-fragmentation chain transfer (RAFT) is a controlled/living polymerization that can synthesize well-defined homopolymers and block copolymers. Numerous RAFT syntheses of PNIPAAm homopolymer<sup>5–12</sup> and block copolymers<sup>9,13–24</sup> containing PNIPAAm have been reported. However, RAFT syntheses of PMAA have been limited to block copolymers of PMAA with poly(benzyl methacrylate) or poly(methyl methacrylate) (PMMA)<sup>25</sup> and random copolymers of poly(MMA-co-MAA).<sup>26,27</sup> Even though block copolymer of PNIPAAm and poly(acrylic acid) (PAA) has been synthesized with RAFT polymerization for possible double-stimuli responsive drug delivery system,<sup>19</sup> and studies on RAFT polymerization kinetics of PNIPAAm<sup>10,11</sup> and poly(acrylic acid)<sup>28</sup> have been reported, to our knowledge, no report on the RAFT synthesis of block copolymers of PNIPAAm and PMAA has been published and a literature review produced no report on the RAFT polymerization kinetics of PMAA. In this article, we provide detailed RAFT polymerization kinetics of PNIPAAm and PMAA using the

Correspondence to: Y.-L. Cheng (ylc@chem-eng.utoronto.ca).

Contract grant sponsors: Natural Sciences and Engineering Research Council of Canada (NSERC); Materials and Manufacturing Ontario (MMO).

only commercially available RAFT agent, carboxymethyl dithiobenzoate (CMDDB) and the effects of RAFT agent concentrations on the polymerization of PNIPAAm. Since each monomers' kinetics is unique, knowledge of polymerization kinetics of PMAA and PNIPAAm would facilitate the synthesis of polymers with desirable characteristics. We also demonstrate the synthesis of diblock copolymers of poly(NIPAAm)-*block*-poly(MAA) copolymers, and triblock copolymers poly(NIPAAm)-*block*-poly(MAA)-*block*-poly(NIPAAm) for the first time. Moreover, we present preliminary evidence that aqueous solutions of the block copolymers show temperature-responsive gelation in a reversible fashion, which has not been demonstrated with previous block copolymers of PNIPAAm and PAA.<sup>19</sup> Thus, this unique combination of temperature reversible gelation and possible angiogenic characteristics of these PNIPAAm and PMAA block copolymers allow for their potential use in a wide range of pharmaceutical, biomedical, and tissue engineering applications such as wound dressing.

## EXPERIMENTAL

### Materials

NIPAAm (ACROS, 99%) was recrystallized twice in 50/50 (v/v) heptane/toluene solvent (Sigma, analytical grade) before polymerization. MAA (Sigma, 99%) was

purified by distillation under reduced pressure prior to use. Carboxymethyl dithiobenzoate (CMDDB) or *S*-(thiobenzoyl)thioglycolic acid (Aldrich, 98%), and polymerization initiator 4,4'-azobis(4-cyanopentanoic acid) (ACP, ACROS, 99%) were used as received. 1,4-dioxane (ACROS, analytical grade), methanol, and diethyl ether (EM Science, analytical grade), *N,N*-dimethylformamide (DMF, Sigma, analytical grade), deuterated dimethyl sulfoxide, DMSO-*d*<sub>6</sub> (ACROS, 99.9%), lithium bromide (LiBr, Sigma, 98%), tetramethylammonium hydroxide (Aldrich, 98%), and methyl iodide (Aldrich, 99%) were all used as received.

### RAFT synthesis of PNIPAAm homopolymer

PNIPAAm homopolymer synthesis [Fig. 1(a)] was carried out as follows: In a three-neck round bottom flask, 6.45 g of NIPAAm (57.08 mmol), 125 mg of CMDDB RAFT agent (0.57 mmol), 40 mg of ACP initiator (0.14 mmol), and 30 mL of 1,4-dioxane were mixed and stirred using a magnetic stir bar. Molar ratio of CMDDB to ACP was kept constant at 4:1; a low concentration of ACP was used to keep the initiation rate low and thus reduce the rate of radical-radical termination. The reagents were dissolved and the solution was purged with high purity helium for 30 min to remove dissolved oxygen. Polymerization was then conducted under helium atmosphere at a constant temperature of 60°C for 64 h with continuous stirring. After 64 h, the reaction

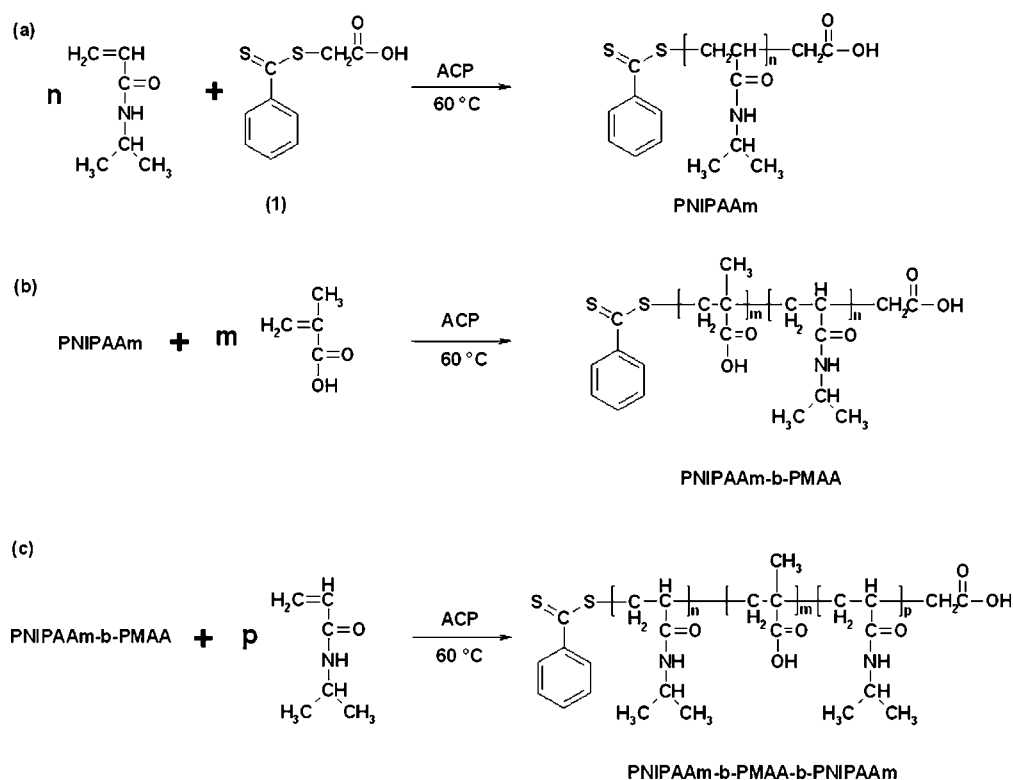


Figure 1 Reaction scheme for RAFT polymerization.

was stopped by diluting the reaction mixture with 1,4-dioxane to 100 mL and cooled to room temperature. The polymer was then purified by precipitation in diethyl ether and dried *in vacuo*. Purified PNIPAAm homopolymers were subsequently used for block copolymer syntheses. As a blank reaction, the procedure was also preformed without CMDDB RAFT agent. For RAFT polymerization kinetics data, samples were withdrawn at predetermined time points and immediately quenched (i.e., stopped) in liquid nitrogen; conversion and molecular weight as a function of time were then determined.

In separate studies, the effects of RAFT agent on NIPAAm polymerization were determined by varying the molar ratio of CMDDB to ACP from 2 to 21 and the molar ratio of NIPAAm to CMDDB from 100 to 400 independently.

#### RAFT synthesis of PMAA homopolymer

A procedure similar to PNIPAAm polymerization was used for PMAA synthesis. 4.85 mL of MAA (4.92 g, 57.24 mmol), 126.5 mg of CMDDB RAFT agent (0.58 mmol), and 42 mg of ACP initiator (0.15 mmol) were dissolved in 30 mL of methanol and purged with helium for 30 min. Polymerization was conducted under helium atmosphere at 60°C for 10 h and purification was performed similarly to PNIPAAm purification. As a blank reaction, polymerization of MAA without CMDDB was carried out using otherwise identical procedures. RAFT polymerization kinetic data for MAA polymerization were obtained in the same manner as for NIPAAm polymerization but the effects of RAFT agent concentration on MAA polymerization were not investigated.

#### RAFT synthesis of diblock poly(NIPAAm)-block-poly(MAA)

For the synthesis of the diblock poly(NIPAAm)-block-poly(MAA) copolymers, RAFT-synthesized PNIPAAm was used as a macromolecular RAFT agent [Fig. 1(b)]. In a three-neck round bottom flask, 732 mg of purified homopolymer of PNIPAAm (0.057 mmol,  $\overline{M}_{n(\text{SEC})} = 12,800$  g/mol, PDI = 1.2), 4 mg of ACP (0.014 mmol), and 0.3 mL of MAA (0.30 g, 3.54 mmol) were dissolved in 15 mL of methanol and purged with helium for 30 min. Polymerization was conducted under helium atmosphere at 60°C for 10 h and finally the diblock copolymers were purified by precipitation in diethyl ether and dried *in vacuo* to remove unreacted monomers.

#### RAFT synthesis of triblock poly(NIPAAm)-block-poly(MAA)-block-poly(NIPAAm)

A procedure similar to diblock polymerization was used except poly(NIPAAm)-block-poly(MAA) was

used as macromolecular RAFT agent instead [Fig. 1(c)]. Forty milligrams of purified block copolymer of poly(NIPAAm)-block-poly(MAA) (2.35  $\mu\text{mol}$ ,  $\overline{M}_{n(\text{SEC})} = 17,200$  g/mol, PDI = 1.3), 1 mg of ACP (3.57  $\mu\text{mol}$ ), and 42 mg of NIPAAm (358  $\mu\text{mol}$ ) were dissolved in 5 mL of methanol and purged with helium for 30 min. Polymerization was conducted under helium atmosphere at 60°C for 18 h, and the triblock copolymer was also purified in diethyl ether and dried *in vacuo* to remove unreacted monomers. The goal of this work was to demonstrate that block copolymers of PNIPAAm and PMAA can be synthesized using RAFT; there was no attempt to determine in detail the effect of synthesis conditions on the lengths of the added blocks in the copolymers.

#### Size exclusion chromatography

Prior to size exclusion chromatography (SEC) analysis, MAA groups were converted to methyl methacrylate esters with tetramethylammonium hydroxide,  $(\text{CH}_3)_4\text{N}^+\text{OH}^-$  and methyl iodide,  $\text{CH}_3\text{I}$  in DMF at 80°C according to reported procedures.<sup>29</sup> SEC was performed on a Waters Associates liquid chromatography system equipped with Waters 510 pump and Waters 410 differential refractometer detector. StyraGel columns (7.8 mm ID  $\times$  300 mm) HR2, HR3, and HR4 with  $10^2$ ,  $10^3$ , and  $10^4$  Å pore sizes were used. DMF with 0.05M LiBr was used as the eluent with 1.0 mL/min flow rate at a temperature of 80°C. The injection volume was 100  $\mu\text{L}$  and polystyrene standards (PS) were used for calibration. Number average molecular weight,  $\overline{M}_{n(\text{SEC})}$  and molecular weight distribution (i.e., polydispersity index,  $\text{PDI} = \overline{M}_w/\overline{M}_n$ ) from SEC chromatograms were calculated relative to PS standards using Waters Associates Millennium 2.10 software.

#### <sup>1</sup>H NMR spectroscopy

<sup>1</sup>H NMR measurements were conducted with a 400 MHz Unity spectrometer using deuterated DMSO- $d_6$  as solvent and tetramethylsilane as internal standard. PNIPAAm was identified by the proton on the amide group ( $-\text{CO}-(-\text{NH})-$ ) at  $\delta \sim 6.9$ –7.5 ppm, while PMAA was identified by the acid proton of the carboxyl group ( $-\text{COOH}$ ) at  $\delta \sim 12.1$ –12.6 ppm. NIPAAm monomers were identified by the vinyl protons at  $\delta \sim 6.1$  ppm and  $\delta \sim 5.5$  ppm, and MAA monomers were identified by the vinyl protons at  $\delta \sim 6.0$  ppm and  $\delta \sim 5.6$  ppm.

For kinetics study, unpurified polymer samples were collected at different reaction times from polymerization runs and analyzed with <sup>1</sup>H NMR at a polymer concentration of  $\sim 30$  mg/mL in DMSO- $d_6$ . Conversion was calculated using the integrated monomer and polymer <sup>1</sup>H NMR peaks illustrated in eq. (1). For PNIPAAm, the  $-\text{NH}$  proton and for PMAA the  $-\text{CH}_3$

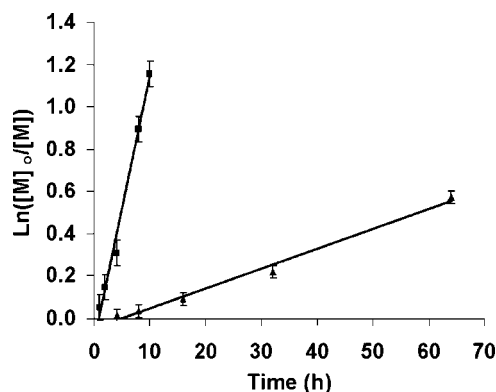


**Figure 2** PNIPAAm and PMAA polymerization kinetics. (▲) PNIPAAm polymerized at 60°C in 1,4-dioxane, [NIPAAm] = 1.90M, [NIPAAm] : [CMDB] : [ACP] = 100 : 1 : 0.25. (■) PMAA polymerized at 60°C in methanol, [MAA] = 1.90M, [MAA] : [CMDB] : [ACP] = 100 : 1 : 0.25.  $n = 3$  for all data points, error bars indicate standard deviations.

protons were used.  $^1\text{H}$  NMR analysis confirmed the absence of unreacted monomer in all purified polymer samples, and the analysis of block copolymers confirmed the presence of both PNIPAAm and PMAA.

### Differential scanning calorimetry

Differential scanning calorimetry (DSC) spectra were recorded on TA Instrument, DSC 2010 at a heating or cooling rate of 2°C/min. The LCST of the homopolymers of PNIPAAm and block copolymers were determined by running DSC scans of the corresponding polymers dissolved in phosphate buffered saline (PBS, pH 7.4) solutions at 5 wt % loaded in ~30  $\mu\text{L}$  volume aluminum hermetic DSC pan. The peak temperatures of the endotherms were taken as the transition temperatures. The samples were also cyclically heated and cooled to determine the reversibility of the thermal transitions.

## RESULTS AND DISCUSSION

### RAFT polymerization kinetics

The kinetics of PNIPAAm and PMAA homopolymer synthesis via RAFT polymerization using CMDB are shown in Figure 2. For both polymers, an induction (or inhibition) period followed by apparent first-order kinetics can be seen. Furthermore, Table I shows that

$$\% \text{ Conversion} = \frac{\text{Integrated polymer peak}}{\text{Integrated polymer peak} + \text{Integrated monomer peak}} \times 100\% \quad (1)$$

the RAFT polymerization kinetics of PNIPAAm and PMAA are both retarded relative to blank reactions in which CMDB were not used. Compared with conventional free-radical polymerization, RAFT polymerization of PMAA was approximately seven times slower (69% conversion at 10 h vs. > 95% conversion at 2 h), and RAFT polymerization of PNIPAAm was more than 11 times slower (44% conversion at 64 h vs. > 95% conversion at 12 h).

The apparent first-order kinetics plots of PNIPAAm and PMAA shown in Figure 2 imply a constant number of propagating radicals, or chain transfer equilibrium conditions, throughout the duration of polymerization. This behavior is commonly observed in free-radical polymerization,<sup>30</sup> and has also been observed in many RAFT polymerizations.<sup>10,31–35</sup>

The reasons for the induction periods and retardation observed for some RAFT polymerization systems

**TABLE I**  
Results of RAFT Polymerization of PNIPAAm, PMAA, and their Copolymers

Synthesis product	Reaction conditions				Product characteristics			
	[Monomer] ( $M \times 10^3$ )	[ACP] ( $M \times 10^3$ )	[RAFT] ( $M \times 10^3$ )	Reaction time (h)	Conversion (%)	$\bar{M}_n(\text{SEC})$ (g/mol)	PDI	LCST (°C)
PMAA	1900 <sup>a</sup>	4.75	19.0 <sup>c</sup>	10	69	13,300	1.3	n/a
PNIPAAm	1900 <sup>b</sup>	4.75	19.0 <sup>c</sup>	64	44	12,800	1.2	31
PNIPAAm- <i>b</i> -PMAA	236 <sup>a</sup>	0.95	3.81 <sup>d</sup>	10	n/a	17,200	1.3	31
PNIPAAm- <i>b</i> -PMAA- <i>b</i> -PNIPAAm	72 <sup>b</sup>	0.71	0.74 <sup>e</sup>	18	n/a	20,700	1.4	31
PNIPAAm (blank)	1900 <sup>b</sup>	4.75	n/a	12	>95	152,700	2.3	31
PMAA (blank)	1900 <sup>a</sup>	4.75	n/a	2	>95	326,500	3.0	n/a

<sup>a</sup> MAA in methanol.

<sup>c</sup> NIPAAm in 1,4-dioxane.

<sup>b</sup> RAFT = CMDB.

<sup>d</sup> RAFT = PNIPAAm macromolecular transfer agent,  $\bar{M}_n(\text{SEC}) = 12,800$  g/mol, PDI = 1.2.

<sup>e</sup> RAFT = PNIPAAm-*b*-PMAA macromolecular transfer agent,  $\bar{M}_n(\text{SEC}) = 17,200$  g/mol, PDI = 1.3.

are not completely understood,<sup>10,36–39</sup> but as shown in Figure 3, slow fragmentation of adduct (2) to produce  $R^*$  radical, slow initiation by the expelled  $R^*$  radical, or side reactions involving the RAFT adducts (2) in the fragmentation/chain transfer step have been suggested as possible explanations.<sup>36</sup> Slow fragmentation of (2) would slow the rate of  $R^*$  formation and the apparent rate of initiation by  $R^*$ , thus resulting in slower polymerization kinetics. Slower fragmentation and  $R^*$  initiation would also give rise to a longer timeframe to reach chain transfer equilibrium, thus resulting in an induction period. CMDB has a poor primary R leaving group ( $-\text{CH}_2\text{CH}_2\text{COOH}$ ), which would result in a slow fragmentation of (2) making this a plausible explanation for the observed kinetics features in PNIPAAm and PMAA polymerization. Induction periods and retardation have been reported in other CMDB-mediated polymerizations and were attributed to the same slow adduct fragmentation mechanism.<sup>40,41</sup> On the other hand, Schilli et al.<sup>10</sup> proposed that the induction peri-

ods observed in the polymerization of NIPAAm using RAFT agents benzyl and cumyl dithiocarbamates were due to slow initiation by the expelled  $R^*$  radicals because  $R^*$  might be involved in transfer reaction with (3) (see Fig. 3).

### Molecular weight and polydispersity

One of the distinct advantages of living radical polymerization, such as RAFT, is the ability to control molecular weight. Theoretical number average molecular weight,  $\bar{M}_{n(\text{ideal})}$ , based on idealized RAFT polymerization conditions was calculated using the following equation.<sup>12</sup>

$$\bar{M}_{n(\text{ideal})} = \frac{[M]_0}{[\text{RAFT}]_0} \times \text{conversion} \times M_i \quad (2)$$

where  $[\text{RAFT}]_0$  is the initial RAFT concentration,  $[M]_0$  is the initial monomer concentration, and  $[M]_i$  is the monomer molecular weight. Equation (2) assumes:

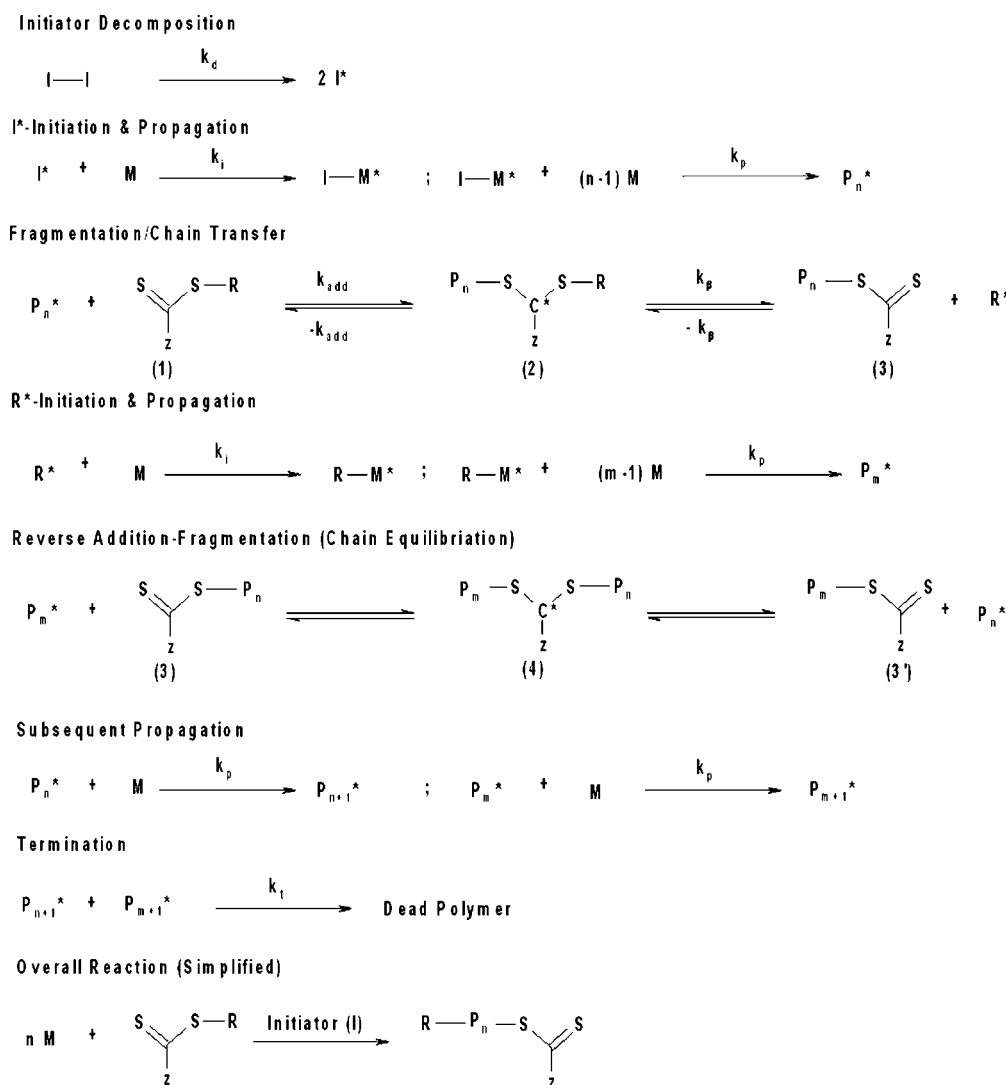
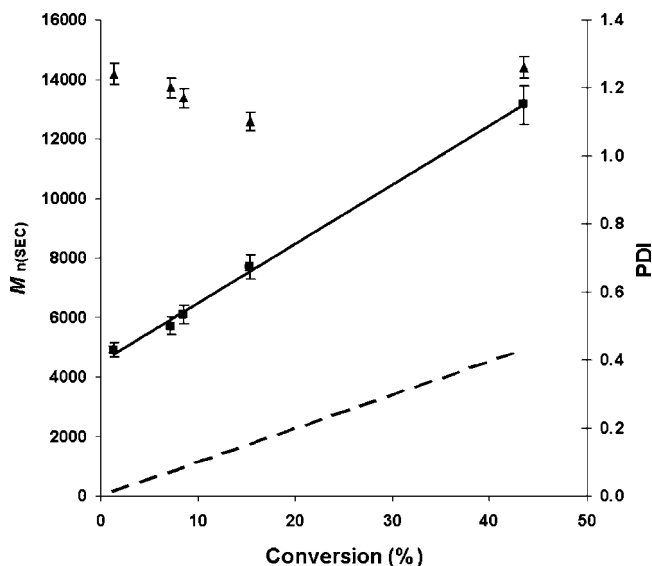


Figure 3 Mechanism of RAFT polymerization.



**Figure 4**  $\bar{M}_n(\text{SEC})$  and PDI vs. conversion plot for PNIPAAm. Polymerization at 60°C in 1,4-dioxane. [NIPAAm] = 1.90M, [NIPAAm] : [CMDB] : [ACP] = 100 : 1 : 0.25. (■) experimental  $\bar{M}_n(\text{SEC})$ , (---) theoretical  $\bar{M}_n(\text{ideal})$  using eq. (2), (▲) PDI.  $n = 3$  for all data points, error bars indicate standard deviations.

(a) the efficiency of the RAFT agent is 100% (i.e., all RAFT agents are attached to a polymer chain end), (b) termination events (chain transfer to monomer and radical–radical termination) are negligible, and (c) the initiation rates of  $\text{I}^*$  are low, therefore does not account for the small number of chains formed from the initiator.<sup>11,36</sup>

Polymerization kinetics results (Figs. 4 and 5) show that  $\bar{M}_n(\text{SEC})$  increases linearly with conversion for both PNIPAAm and PMAA, as expected. However, neither  $\bar{M}_n(\text{SEC})$  plots went through the origin and both were significantly higher than the calculated  $\bar{M}_n(\text{ideal})$ .

The linearity of the  $\bar{M}_n(\text{SEC})$  vs. conversion indicates a constant number of propagating chains and hence the absence of irreversible transfer reactions; it is also suggestive of the living nature of RAFT polymerization.<sup>10,42</sup> The apparent rapid polymerization kinetics at early times resulting in higher initial molecular weights at low conversions and the poor correlation between  $\bar{M}_n(\text{SEC})$  and  $\bar{M}_n(\text{ideal})$  observed for both PNIPAAm and PMAA may be attributed to the slow fragmentation of CMDB and the resulting low transfer constant of CMDB. The propagating radical chain of PNIPAAm or PMAA,  $\text{P}_n^*$  is bulkier and more stabilized than the carboxymethyl radical leaving group,  $\text{R}^*$ , of CMDB (Fig. 3). Therefore, in the early stages of polymerization, the fragmentation equilibrium of the intermediate radical adduct (2) will be displaced to yield CMDB, (1) and a PNIPAAm or PMAA propagating radical,  $\text{P}_n^*$  rather than leading to the formation of a dormant chain (3) and a carboxymethyl radical,  $\text{R}^*$ , in the fragmentation/chain transfer step in

Figure 3. This gives rise to slow CMDB consumption and consequent slow formation of new chains by  $\text{R}^*$ . During this early stage, the first  $\text{I}^*$ - and  $\text{R}^*$ -initiated chains propagate without significant participation in the molecular weight-controlling RAFT chain equilibration step, thus giving rise to a high rate of molecular weight growth with conversion. As more CMDB is consumed and recruited into the  $\text{R}^*$  initiation/propagation and subsequent RAFT chain equilibration steps, the rate of molecular weight growth with conversion slows to RAFT-mediated levels. With constant numbers of RAFT propagating centers, molecular weight increases linearly with conversion. Similar findings were reported by others working with CMDB as RAFT agent.<sup>24,35,41,43</sup>

Moreover, CMDB is an inefficient RAFT agent because of its low chain transfer constant; thus the assumption of 100% effective RAFT agent underlying eq. (2) is invalid, which leads to a positive deviation of  $\bar{M}_n(\text{SEC})$  from  $\bar{M}_n(\text{ideal})$ .<sup>44</sup> Thus, the higher initial molecular weight and the lack of agreement between  $\bar{M}_n(\text{SEC})$  and  $\bar{M}_n(\text{ideal})$  can be attributed to the low transfer constant of CMDB. Other researchers have also pointed to the low CMDB transfer constant as the reason for similar  $\bar{M}_n$  vs. conversion observations in the polymerization of other polymers.<sup>24,35,41,43</sup>

RAFT-mediated molecular weight distribution control is also shown in Figures 4 and 5 for PNIPAAm and PMAA, respectively. For both polymers, PDI first decreases with conversion to reach low values: 1.1 at 15% conversion for PNIPAAm and 1.3 at 27% conversion for PMAA. As conversion further increases, PDI

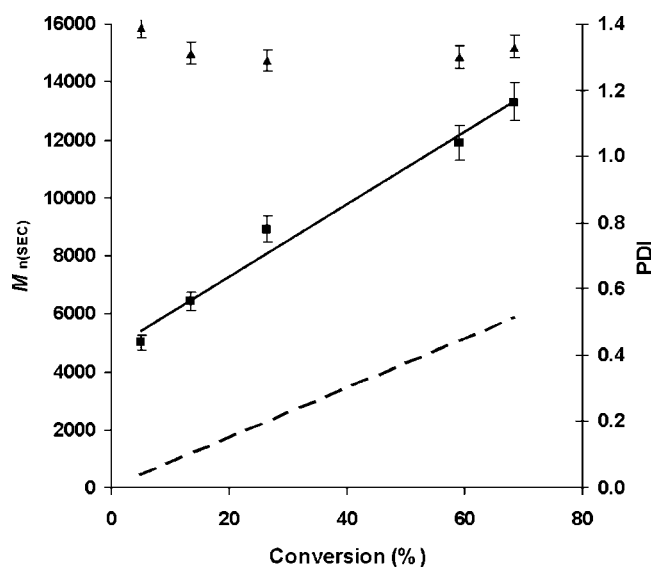


**Figure 5**  $\bar{M}_n(\text{SEC})$  and PDI vs. conversion plot for PMAA. Polymerization at 60°C in methanol. [MAA] = 1.90M, [MAA] : [CMDB] : [ACP] = 100 : 1 : 0.25. (■) experimental  $\bar{M}_n(\text{SEC})$ , (---) theoretical  $\bar{M}_n(\text{ideal})$  using eq. (2), (▲) PDI.  $n = 3$  for all data points, error bars indicate standard deviations.

also increases, contradicting the prediction of idealized RAFT kinetics. For both polymers, however, PDI stayed well below the theoretical free-radical polymerization limit of 1.5 for termination by combination. As well, polydispersities of RAFT-synthesized polymers were much lower than RAFT-free controls (Table I), further suggestive of the living characteristics of RAFT.<sup>36</sup>

In idealized RAFT kinetics,<sup>45</sup> PDI is expected to decrease with conversion. Before RAFT-mediated chain equilibration occurs, PDI is dictated by conventional radical polymerization processes, giving rise to a high PDI. Then as RAFT-mediated chain equilibration is established, control over molecular weight occurs and a decrease in PDI is expected. The observed increase in PDI at higher conversion may be attributed to an increased probability of termination reactions as the monomer becomes increasingly depleted.<sup>41</sup> Viscosity increase at high conversions would also favor heterogeneous growth of polymer chains, further contributing to the increase in polydispersities. Similar increase in polydispersity with conversion has been reported for the RAFT polymerization of NIPAAm.<sup>10,11</sup> Termination either by transfer to monomer or disproportionation,<sup>11</sup> or the combination of growing chains at high conversion<sup>10</sup> were possible explanations that have been cited for the increasing polydispersity with conversion.

Moreover, CMDB degradation during polymerization was observed that might further contribute to the increase in PDI at high conversion. Thiocarbonylthio moieties are highly colored, and the presence of CMDB renders the polymerization solution reddish. A slow reduction in the intensity of the reddish color in the polymerization medium was observed as polymerization progressed. In some experiments, the discoloration was very significant at higher conversion, when PDI was found to increase. The discoloration can be directly related to the degradation of CMDB, or a progressive disappearance of the chromophoric dithioester chain ends.<sup>41</sup> The degradation of CMDB will reduce the concentration of active RAFT agent, and would be expected to contribute to the increase in PDI observed in this study.

#### Effects of [monomer] : [RAFT] ratio

Idealized RAFT kinetics analysis (eq. (2)) suggests that molecular weight can be controlled by the ratio of  $[M]_0 : [RAFT]_0$ , and would increase linearly with conversion. As seen in Figure 6, the observed PNIPAAm  $\bar{M}_n$  normalized by conversion, conforms to the expected linear dependence on  $[NIPAAm]_0 : [CMDB]_0$  as both  $[CMDB]_0$  and  $[ACP]_0$  were held constant. This result shows that  $\bar{M}_n$  can be controlled in a predictable way by changing the ratio of  $[M]_0 : [RAFT]_0$ . It should be noted that the slope of the plot in Figure 6 (250 g/mol) does not equal the monomer molecular weight of NIPAAm (113 g/mol) as eq. (2)

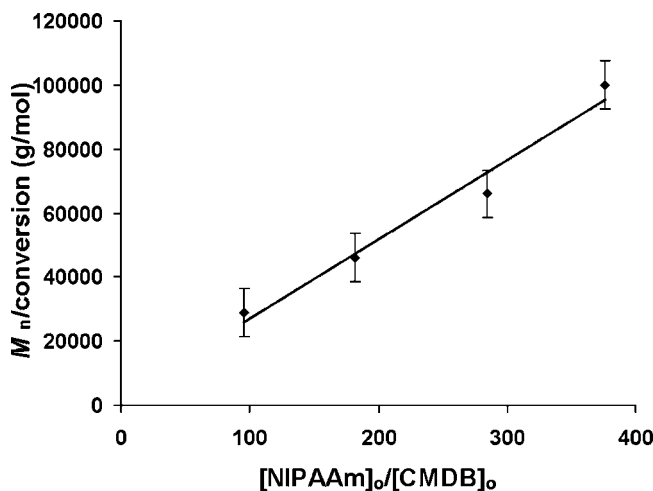


**Figure 6** Effects of  $[NIPAAm]_0 : [CMDB]_0$  on  $\bar{M}_n$ . Polymerization at 60°C in 1,4-dioxane for 64 h.  $[CMDB] = 10.53 \times 10^{-3} M$ ,  $[CMDB] : [ACP] = 4$ .  $n = 2$ , error bars show the range of data values.

suggests; further indicating the invalidity of the assumption underlying eq. (2).

Decreasing  $[ACP]_0$  while holding  $[NIPAAm]_0$  and  $[CMDB]_0$  constant, or increasing the ratio of  $[CMDB]_0 : [ACP]_0$  might be a better strategy for controlling molecular weight and narrowing molecular weight distribution (i.e., lowering PDI), since one of the key factors in successfully producing narrow molecular weight distribution with RAFT polymerization is to minimize the initiator-derived chains.<sup>36</sup> However, decreasing the number of initiator-derived chains will slow polymerization kinetics. As expected, increasing the ratio of  $[CMDB]_0 : [ACP]_0$  from 2 to 21, while keeping the  $[NIPAAm]_0$  and  $[CMDB]_0$  concentration constant, resulted in a decrease in conversion from 52 to 8%, for fixed polymerization times.  $\bar{M}_{n(SEC)}$  and PDI both decreased from 16,700 to 7052 g/mol and 1.3 to 1.1, respectively, with increasing values of  $[CMDB]_0 : [ACP]_0$  from 2 to 21. Since the concentration of CMDB relative to propagating chains increases with increasing values of  $[CMDB]_0 : [ACP]_0$ , propagating chains participate more frequently in the RAFT chain equilibration step, leading to slower chain growth and reduce termination reactions to produce lower molecular weight and lower PDI polymers. Thus, the RAFT process can control the molecular weight distribution (i.e., polydispersity), and the increase in RAFT concentration relative to initiator concentration lowers PDI, but at the same time slowing kinetics, and reducing  $\bar{M}_n$ .

#### Block copolymers of PNIPAAm and PMAA

The RAFT process is a living radical polymerization that can be used to synthesize block copolymers. Furthermore, RAFT has the distinct advantage of being applicable to acidic monomers such as MAA with no

extra protection step. These characteristics were exploited to synthesize block copolymers of PNIPAAm and PMAA. RAFT synthesized and purified PNIPAAm was chain extended with MAA to make diblock poly(NIPAAm)-*block*-poly(MAA) copolymers. The purified diblock copolymers were then further chain extended with NIPAAm to form poly(NIPAAm)-*block*-poly(MAA)-*block*-poly(NIPAAm) triblock copolymers.

SEC chromatograms of PNIPAAm, diblock and triblock copolymers are shown in Figure 7. A single peak was observed for each of the polymers, and a decrease in retention time as well as progressive peak broadening is seen with each block addition. As summarized in Table I,  $\bar{M}_n(\text{SEC})$  and PDI of the three polymers were found to be in accordance with the observed retention times and peak broadening. The broadening of molecular weight distribution (i.e., increase in PDI) may be attributed to the presence of dead chains that do not contain RAFT ends and do not participate in chain extension, the low mobility of the macromolecular chain transfer radical of the homopolymer PNIPAAm and diblock, resulting in even lower transfer constants,<sup>43</sup> and perhaps a small degree of homopolymer formation at each stage of chain extension. In the absence of chain transfer to

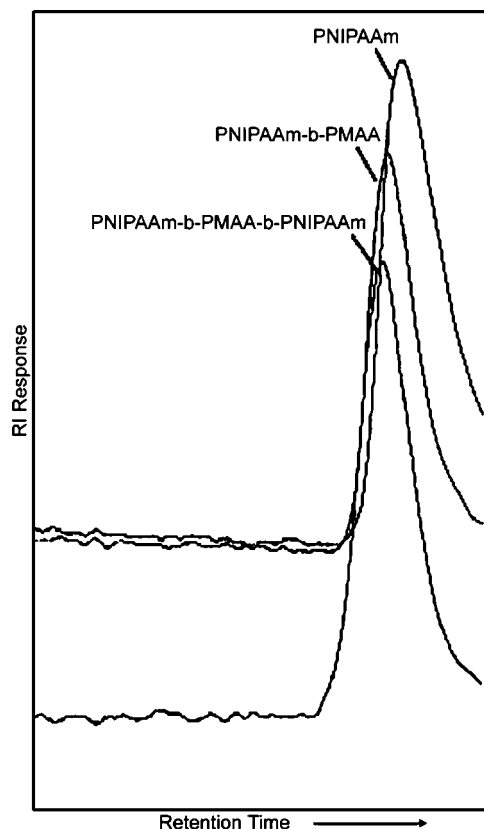


**Figure 7** SEC chromatogram of PNIPAAm, poly(NIPAAm)-*block*-poly(MAA) and poly(NIPAAm)-*block*-poly(MAA)-*block*-poly(NIPAAm).

solvent, initiator, or monomer, the total number of chains formed will be equal to or less than the moles of RAFT agent used plus the moles of initiator-derived radicals generated during the course of the polymerization. In the synthesis of the second and third blocks, these additional initiator-derived chains are a source of homopolymer impurity.<sup>25</sup>

<sup>1</sup>H NMR evidence that further supports successful chain extension is shown in Figure 8. Figure 8(a) shows the characteristic polymer amide peak ( $\delta \sim 6.9\text{--}7.6$  ppm, CO-(NH-)) of homopolymer PNIPAAm, while in Figure 8(b), the block copolymer poly(NIPAAm)-*block*-poly(MAA) not only shows the characteristic PNIPAAm peaks but also the characteristic acid peak of PMAA ( $\delta \sim 12.1\text{--}12.6$  ppm, -COOH). The combination of a single SEC peak and the presence of characteristic protons for both PNIPAAm and PMAA leads to the conclusion that diblock poly(NIPAAm)-*block*-poly(MAA) copolymer was successfully synthesized. Similarly, <sup>1</sup>H NMR results also confirm the composition of PNIPAAm and PMAA in the triblock copolymers (data not shown).

### Thermal properties

Figure 9 shows the DSC scans of 5 wt % solutions of PNIPAAm, the diblock copolymer, and the triblock copolymer in phosphate buffered saline (PBS, pH 7.4) solution. At a heating rate of 2°C/min, all three solutions showed an endothermic peak at  $\sim 31^\circ\text{C}$ , in agreement with well-reported values of LCST for PNIPAAm.<sup>1</sup> Cyclic heating and cooling of all three solutions showed that the LCST transitions are reversible with virtually no hysteresis (data not shown).

Moreover in Figure 9, broadening of the endotherm from homopolymer PNIPAAm to block copolymers can be seen. The broad endothermic transition of the block copolymers might be the result of hydrogen bonding interactions between PNIPAAm and PMAA blocks. Both polymers have the ability to donate and accept protons and are known to form intermolecular complexes by hydrogen bonding in aqueous medium.<sup>46,47</sup> Hydrogen bonding will reduce the mobility of the copolymer chains leading to a gradual transition indicated by the broadening of the endothermic peak. Broad endothermic transition for PNIPAAm hydrogels with increased crosslink density,<sup>48</sup> restricted mobility on silica surface,<sup>49</sup> and containing comonomer acrylic acid<sup>50</sup> or methacrylic acid<sup>51,52</sup> have also been reported.

Preliminary visual observations are consistent with DSC findings. Upon heating 5 wt % solutions of either the diblock or triblock copolymer in PBS (pH 7.4) (1.5 cm diameter, 0.5 cm height) to 37°C, the solutions gelled (i.e., does not flow under the influence of gravity) in less than 1 min. Gelation was found to be thermally reversible. Reversible gelling of the block copolymers might



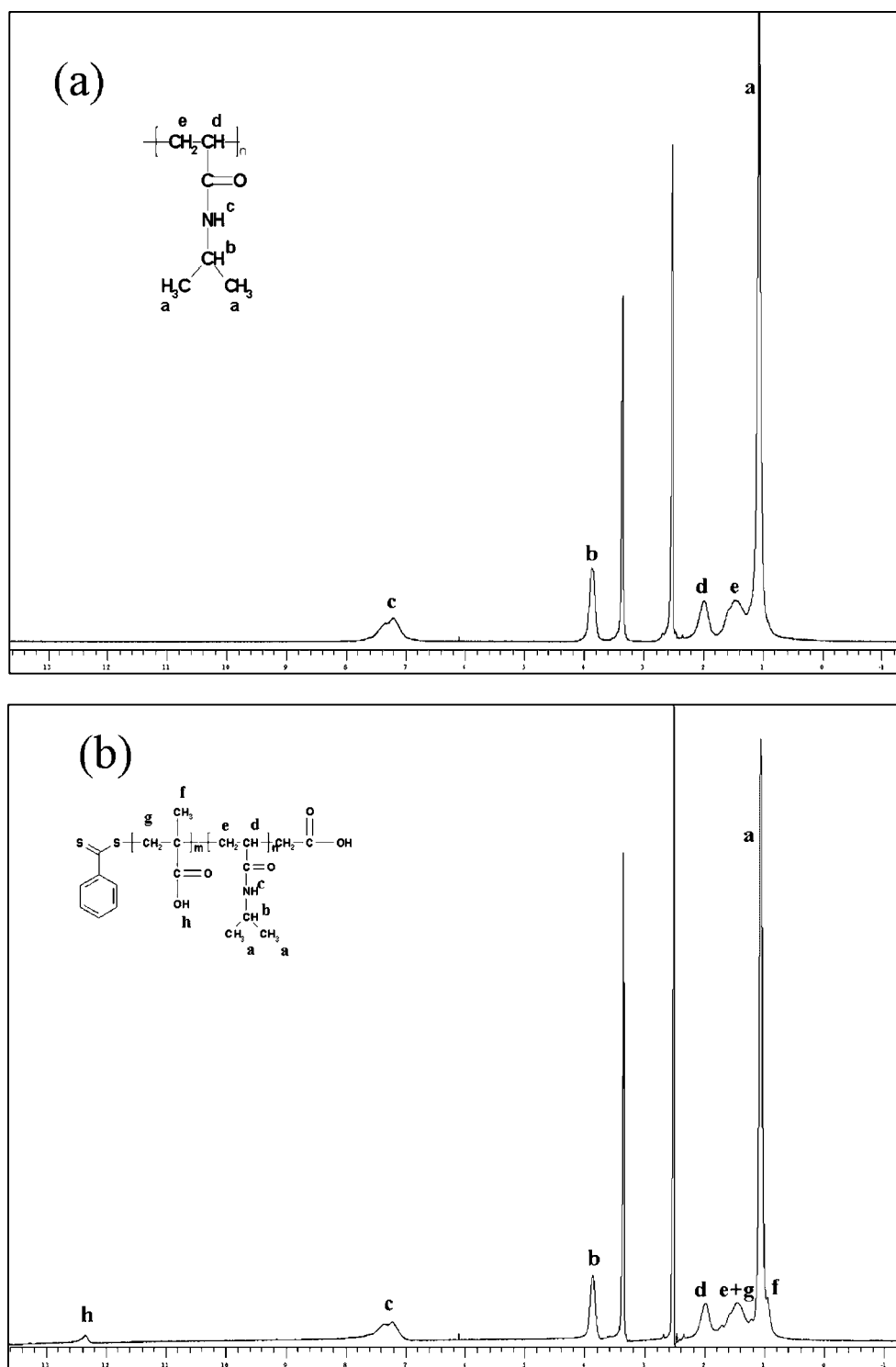
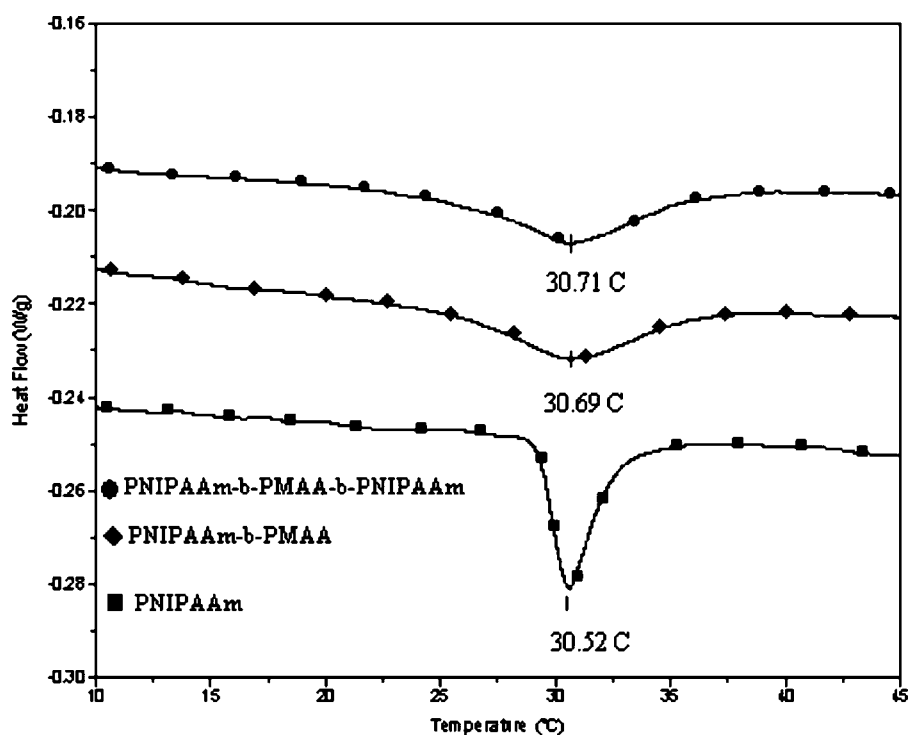


Figure 8  $^1\text{H}$  NMR Spectrum of (a) PNIPAAm; (b) poly(NIPAAm)-block-poly(MAA).

have the advantage of being able to switch back and forth between a solution mixture and a solid gel under specific conditions, allowing easy application, removal or reshaping, and without the need for extra additives such as crosslinkers to enable copolymer gelation. Upon heating, diblock poly(NIPAAm)-block-poly(MAA) copolymer is expected to form micelles and the

formation of gel is due to self-assembling micelle packing and entanglement, while the triblock copolymer is expected to form physical crosslinks between PNIPAAm segments of different chains, to form a physically crosslinked gel.<sup>4</sup> To assess the potential use of these copolymers as gelable biomedical, pharmaceutical, and tissue engineering materials, future



**Figure 9** DSC Endotherms of PNIPAAm, poly(NIPAAm)-*block*-poly(MAA), and poly(NIPAAm)-*block*-poly(MAA)-*block*-poly(NIPAAm).

work will explore the detailed dependence of gelation and mechanical properties on temperature, concentrations, as well as block copolymer structure and molecular weight. Also, the block copolymers ability to promote local angiogenesis (blood vessels formation) at implantation site *in vivo* will be investigated in future studies.

## CONCLUSIONS

PNIPAAm and PMAA homopolymers, diblock copolymers, and triblock copolymers were successfully synthesized using RAFT polymerization. The experimental evidence demonstrated living polymerization characteristics, including: linear increase of  $\bar{M}_n$  with conversion, controlled molecular weights, relatively narrow molecular weight distributions, and polymers that can be re-activated to produce block copolymers.

The ratio of monomer to RAFT agent concentrations played an important role in controlling molecular weight and PDI:  $\bar{M}_n$  increases linearly with increasing ratio of monomer to RAFT agent. On the other hand, conversion,  $\bar{M}_n$ , and PDI decreased with increasing ratio of RAFT agent to initiator. CMDDB, the RAFT agent used in this study proved to have a relatively low chain transfer constant, and showed degradation during polymerization, thus contributing to deviations from ideal RAFT kinetics.

Solution of the PMAA and PNIPAAm block copolymers in PBS showed LCST and reversible physical

transformations between solution and gel forms at  $\sim 31^\circ\text{C}$ . The thermoreversible gelation property of the block copolymers makes these block copolymers promising candidates for a wide range of pharmaceutical, biomedical and engineering applications.

## References

- Schild, H. G. *Prog Polym Sci* 1992, 17, 163.
- Sefton, M. V.; Babensee, J. E.; May, M. H. WO. Pat. 9,716,176 (1996).
- Yuan, J. J.; Ma, R.; Gao, Q.; Wang, Y. F.; Cheng, S. Y.; Feng, L. X.; Fan, Z. Q.; Jiang, L. *J Appl Polym Sci* 2003, 89, 1017.
- Lin, H.-H.; Cheng, Y.-L. *Macromolecules* 2001, 34, 3710.
- Carter, S.; Hunt, B.; Rimmer, S. *Macromolecules* 2005, 38, 4595.
- Kujawa, P.; Watanabe, H.; Tanaka, F.; Winnik, F. M. *Eur Phys J E Soft Matter* 2005, 17, 129.
- Ray, B.; Isobe, Y.; Matsumoto, K.; Habaue, S.; Okamoto, Y.; Kamigaito, M.; Sawamoto, M. *Macromolecules* 2004, 37, 1702.
- Shan, J.; Nuopponen, M.; Jiang, H.; Kauppinen, E.; Tenhu, H. *Macromolecules* 2003, 36, 4526.
- Schilli, C.; Mueller, A. H. E.; Rizzardo, E.; Thang, S. H.; Chong, B. Y. K. *Polym Prepr* 2002, 43, 687.
- Schilli, C.; Lanzendoerfer, M. G.; Mueller, A. H. E. *Macromolecules* 2002, 35, 6819.
- Ganachaud, F.; Monteiro, M. J.; Gilbert, R. G.; Dourges, M. A.; Thang, S. H.; Rizzardo, E. *Macromolecules* 2000, 33, 6738.
- Rizzardo, E.; Chiefari, J.; Chong, Y. K.; Ercle, F.; Krstina, J.; Jeffery, J.; Le, T. P. T.; Mayadunne, R. T.; Meijs, G. F.; Moad, C. L.; Moad, G.; Thang, S. H. *Macromol Symp* 1999, 143, 291.
- Liu, B.; Perrier, S. *J Polym Sci Part A: Polym Chem* 2005, 43, 3643.
- Liu, Q.; Zhang, P.; Lu, M. *J Polym Sci Part A: Polym Chem* 2005, 43, 2615.
- Mertoglu, M.; Garnier, S.; Laschewsky, A.; Skrabania, K.; Storsberg, J. *Polymer* 2005, 46, 7726.

16. Convertine, A. J.; Myrick, L. J.; Lowe, A. B.; McCormick, C. L. *Polym Prepr* 2004, 45, 293.
17. Hong, C. Y.; You, Y. Z.; Pan, C. Y. *J Polym Sci Part A: Polym Chem* 2004, 42, 4873.
18. Kulkarni, S.; Schilli, C.; Mueller, A. H. E.; Hoffman, A. S.; Stayton, P. S. *Bioconjugate Chem* 2004, 15, 747.
19. Schilli, C. M.; Zhang, M.; Rizzardo, E.; Thang, S. H.; Chong, Y. K.; Edwards, K.; Karlsson, G.; Mueller, A. H. E. *Macromolecules* 2004, 37, 7861.
20. Ying, L.; Yu, W. H.; Kang, E. T.; Neoh, K. G. *Langmuir* 2004, 20, 6032.
21. You, Y.; Hong, C.; Wang, W.; Lu, W.; Pan, C. *Macromolecules* 2004, 37, 9761.
22. Yusa, S.; Shimada, Y.; Mitsukami, Y.; Yamamoto, T.; Morishima, Y. *Macromolecules* 2004, 37, 7507.
23. Schilli, C. M.; Mueller, A. H. E.; Rizzardo, E.; Thang, S. H. Chong, Y. K. *ACS Symp Ser* 2003, 854, 603.
24. Krasia, T.; Soula, R.; Boerner, H. G.; Schlaad, H. *Chem Commun* 2003, 538.
25. Chong, B. Y. K.; Le, T. P. T.; Moad, G.; Rizzardo, E.; Thang, S. H. *Macromolecules* 2001, 34, 32.
26. Sprong, E.; Wet-Roos, D.; Tonge, M.; Sanderson, R. *J Polym Sci Part B: Polym Phys* 2004, 42, 2502.
27. Sprong, E.; Wet-Roos, D.; Tonge, M. P.; Sanderson, R. D. *J Polym Sci Part A: Polym Chem* 2002, 40, 223.
28. Loiseau, J.; Doeerr, N.; Suau, J. M.; Egraz, J. B.; Llauro, M. F.; Ladaviere, C.; Claverie, J. *Macromolecules* 2003, 36, 3066.
29. Greeley, R. H. *J Chromatogr* 1974, 88, 229.
30. Odian, G. *Principles of Polymerization*; Wiley-Interscience: New York, 1991; p 205.
31. Chong, Y. K.; Krstina, J.; Le, T. P. T.; Moad, G.; Postma, A.; Rizzardo, E.; Thang, S. H. *Macromolecules* 2003, 36, 2256.
32. Severac, R.; Lacroix-Desmazes, P.; Boutevin, B. *Polym Int* 2002, 51, 1117.
33. Goto, A.; Sato, K.; Tsujii, Y.; Fukuda, T.; Moad, G.; Rizzardo, E.; Thang, S. H. *Macromolecules* 2001, 34, 402.
34. Kanagasabapathy, A.; Sudalai, A.; Benicewicz, B. C. *Macromol Rapid Commun* 2001, 22, 1076.
35. Mitsukami, Y.; Donovan, M. S.; Lowe, A. B.; McCormick, C. L. *Macromolecules* 2001, 34, 2248.
36. Moad, G.; Chiefari, J.; Chong, B. Y. K.; Krstina, J.; Mayadunne, R. T.; Postma, A.; Rizzardo, E.; Thang, S. H. *Polym Int* 2000, 49, 993.
37. Saricilar, S.; Nott, R.; Barner-Kowollik, C.; Davis, T. P.; Heuts, J. P. A. *Polymer* 2003, 44, 5169.
38. Perrier, S.; Barner-Kowollik, C.; Quinn, J. F.; Vena, P.; Davis, T. P. *Macromolecules* 2002, 35, 8300.
39. Prescott, S. W.; Ballard, M. J.; Rizzardo, E.; Ballard, M. J. *Macromolecules* 2002, 35, 5417.
40. Ladaviere, C.; Dorr, N.; Claverie, J. P. *Macromolecules* 2001, 34, 5370.
41. Favier, A.; Charreyre, M. T.; Chaumont, P.; Pichot, C. *Macromolecules* 2002, 35, 8271.
42. Chiefari, J.; Chong, Y. K.; Ercle, F.; Krstina, J.; Jeffery, J.; Le, T. P. T.; Mayadunne, R. T. *Macromolecules* 1998, 31, 5559.
43. Kanagasabapathy, A.; Claverie, J. P.; Uzulina, I. *Polym Prepr* 1999, 40, 1080.
44. Moad, G.; Rizzardo, E.; Thang, S. H. *Polym Prepr* 2002, 43, 114.
45. Le, T. P.; Moad, G.; Rizzardo, E.; Thang, S. H. *WO. Pat.* 9,801,478 (1997).
46. Diez-Pena, E.; Quijada-Garrido, I.; Barrales-Rienda, J. M.; Wilhelm, M.; Spiess, H. W. *Macromol Chem Phys* 2002, 203, 491.
47. Chen, G.; Hoffman, A. S. *Nature* 1995, 373, 49.
48. Zlatanovic, A.; Petrovic, Z. *Ann Tech Conf Soc Plast Eng* 2001, 59, 3319.
49. Schonhoff, M.; Larsson, A.; Welzel, P. B.; Kuckling, D. *J Phys Chem B* 2002, 106, 7800.
50. Feil, H.; Bae, Y. H.; Feijen, J.; Kim, S. W. *Macromolecules* 1993, 26, 2496.
51. Zhou, S.; Chu, B. *J Phys Chem B* 1998, 102, 1364.
52. Kono, K.; Okabe, H.; Morimoto, K.; Takagishi, T. *J Appl Polym Sci* 2000, 77, 2703.